Drug Design, Development and Therapy

Dovepress
open access to scientific and medical research

Open Access Full Text Article

ORIGINAL RESEARCH

Chrysophanol Inhibits the Progression of Diabetic Nephropathy via Inactivation of TGF-β Pathway

This article was published in the following Dove Press journal:
Drug Design, Development and Therapy

Chuan Guo[1,2]
Yarong Wang[1]
Yuanlin Piao[1]
Xiangrong Rao[2]
Dehai Yin[1]

[1]Department of Traditional Chinese Medicine, Peking Union Medical College Hospital, Peking Union Medical College, Chinese Academy of Medical Science, Beijing 100730, People's Republic of China; [2]Department of Nephropathy, Guang'anmen Hospital, China Academy of Chinese Medical Sciences, Beijing 100053, People's Republic of China

Background: Diabetic nephropathy (DN) is a common form of diabetic complication which threatens the health of patients with diabetes. It has been reported that chrysophanol (CHR) can alleviate the progression of diabetes; however, the role of CHR in DN remains unclear.
Methods: To mimic DN in vitro, human podocytes (AB8/13 cells) were treated with high glucose (HG). Meanwhile, Western blot was performed to detect protein expressions. CCK-8 assay was used to test cell viability and cell proliferation was detected by Ki-67 staining. In addition, flow cytometry was performed to investigate cell apoptosis and cycle and cell migration was tested by transwell assay. Moreover, in vivo model of DN was established to detect the effect of CHR on DN in vivo.
Results: HG-induced AB8/13 cell growth inhibition was significantly rescued by CHR. In addition, HG notably promoted the migration of AB8/13 cells, while this phenomenon was obviously reversed by CHR. Moreover, CHR inhibited the progression of DN via inactivation of TGF-β/EMT axis. Furthermore, CHR alleviated the symptom of DN in vivo.
Conclusion: CHR significantly alleviated the progression of DN via inactivation of TGF-β/EMT signaling in vitro and in vivo. Our findings were helpful to uncover the mechanism by which CHR regulates DN, as well as inspire the development of novel therapy against DN.
Keywords: diabetic nephropathy, chrysophanol, TGF-β, EMT

Introduction

Diabetic nephropathy (DN) is a frequent type of diabetic complication which results from permanent uncontrolled diabetes, and it usually causes end-stage renal diseases (ESRD).[1,2] In addition, DN also results in increased thickness of the basement membrane, glomerular sclerosis and renal fibrosis.[3,4] Nowadays, the main treatment of DN is drug therapy,[5] while the effect of drug therapy remains limited. Thus, it is necessary to explore new strategies for the treatment of DN.

Chrysophanol (CHR, 1,8-dihydroxy-3-methyl-anthraquinone) is a natural product originated from *Rheum undulatum* L. Some reports have indicated that CHR has various physiological functions including anti-tumor and anti-inflammatory.[6,7] Meanwhile, a previous study confirmed that CHR can inhibit the progression of diabetes.[8] In addition, it has reported that CHR can alleviate myocardial injury induced by diabetes. However, the role of CHR in DN remains unclear.

TGF-β has been reported to promote fibronectin and collagen production by transcriptional activation of the relevant genes.[9] Recent reports have indicated that TGF-β acts as a key mediator in the progression of DN.[10,11] Meanwhile, Epithelial-Mesenchymal Transition (EMT) has been regarded as a key mediator in embryonic development and tumor metastasis. In addition, a recent study has reported that

Correspondence: Dehai Yin
Department of Traditional Chinese Medicine, Peking Union Medical College Hospital, Peking Union Medical College, Chinese Academy of Medical Science, No. 1 Shuaifuyuan, Beijing 100730, People's Republic of China
Email yindehai123@126.com

submit your manuscript | www.dovepress.com
DovePress
http://doi.org/10.2147/DDDT.S274191

activation of EMT process in podocytes could lead to the development of DN.[12] Furthermore, it has been reported that upregulation of TGF-β signaling pathway could promote EMT process in the progression of DN.[13] Based on these backgrounds, TGF-β/EMT plays an important role in DN.

In the current study, we aimed to investigate the effect of CHR on the progression of DN and explore the underlying mechanism. We hope our finding may shed new lights on the treatment of DN.

Materials and Methods

Reagents

Chrysophanol and other reagents were obtained from Sigma- Aldrich (Saint Louis, MO, USA).

Cell Culture and Treatments

The human podocytes (AB8/13) was obtained from American Type Culture Collection (ATCC, Manassas, VA, USA) and cultured in RPMI 1640 Medium supplemented with 10% fetal bovine serum (Thermo Fisher Scientific, Waltham, MA, USA), 100 μg/mL streptomycin and 100 U/mL penicillin at 37°C with 5% CO_2. To mimic DN in vitro, AB8/13 cells were treated with 30 mM high glucose (HG, Sigma- Aldrich, Saint Louis, MO, USA) for 48 h.

Cell Counting Kit (CCK)-8 Assay

CCK-8 kit (Dojindo Laboratories, Tokyo, Japan) was used to detect the cell proliferation following the manufacturer's instructions. The cells (1 x 10^4) were seeded into 96-well plates and cultured overnight. After indicated treatments, 10 μL CCK-8 reagents were added into each well and then further incubated for another 2 h. The optical density at 450 nm was measured using a microplate reader (Bio-Rad Laboratories, Richmond, CA, USA).

Immunofluorescence Staining

Immunofluorescence staining for Ki-67 was also conducted to evaluate the cell proliferation. After washing with phosphate buffer saline (PBS) for 3 times, the cells were fixed in 4% paraformaldehyde at 4°C for 30 min. Then, cells were permeabilized with 0.2% Triton X-100 in PBS for 5 min. Potential non-specific binding sites blocked with 3% bovine serum albumin (BSA) in PBS for 1 h at room temperature. Next, cells were incubated with primary antibodies for Ki-67 (1:300, Abcam, Cambridge, MA, USA). Subsequently, cells were incubated with goat anti-rabbit secondary antibody (1:500, Thermo Fisher Scientific, Alexa Fluor 488), at 37°C for 1 h. The nuclei were stained with 4′,6-diamidino-2-phenylindole (DAPI, 1:300, Abcam) overnight at 4°C. The samples were immediately observed by fluorescence microscope (Zeiss, Heidenheim, Germany).

Cell Migration Assay

The 8 mm pore transwell chambers (Corning, New York, NY, USA) were used to determine the rate of cell migration. Cell culture medium containing 4×10^5 cells/200 μL were added into the upper chamber. Meanwhile, the cell culture medium supplemented with 10% FBS was added to the lower chamber of the well. After culturing for 48 h, the migrated cells were fixed with 4% paraformaldehyde, followed by staining with 4% crystal violet. Migrated cells were counted under a light microscope.

Enzyme-Linked Immunosorbent Assay (ELISA)

The levels of interleukin-6 (IL-6), interleukin-1β (IL-1β) and tumor necrosis factor-α (TNF-α) in supernatants of podocytes were detected using ELISA kits from R&D Systems (Minneapolis, MN, USA).

Western Blot Assay

After specific treatment, cells were harvested and lysed using RIPA buffer (Beyotime, Shanghai, China). The concentration of total protein was determined by BCA Protein Assay Kit (Beyotime). Equal amounts of the total protein (20 μg) were separated on 10% polyacrylamide gel electrophoresis (SDS-PAGE) gels followed by transferred onto polyvinylidene fluoride (PVDF) membranes (Millipore, Billerica, MA, USA). After that, the membranes were blocked with 5% skim milk for 1 h at room temperature. Then, the membranes were probed with primary antibodies against E-cadherin (1:1000, Abcam), N-cadherin (1:1000, Abcam), α-smooth muscle aorta (α-SMA, 1:1000, Abcam), Collagen III (1:1000, Abcam), Fibronectin (1:1000, Abcam), phosphorylated drosophila mothers against decapentaplegic 2 (p-Smad2; 1:1000, Abcam), drosophila mothers against decapentaplegic 2 (Smad2; 1:1000, Abcam), phosphorylated drosophila mothers against decapentaplegic 3 (p-Smad3; 1:1000, Abcam), drosophila mothers against decapentaplegic 3 (Smad3; 1:1000, Abcam), p53 (1:1000, Abcam), cyclin-dependent kinase 2 (CDK2; 1:1000, Abcam), BCL2-Associated

X (Bax; 1:1000, Abcam), Cleaved caspase 3 (1:1000, Abcam), and X-linked inhibitor of apoptosis protein (XIAP; 1:1000, Abcam) overnight at 4°C. Then, the membranes were incubated with anti-rabbit secondary antibodies (1:2000, Abcam) for 2 h. The immune blots were visualized using electrochemiluminescence (ECL) reagent (Beyotime). β-actin was used as an internal control.

Apoptosis and Cell Cycle Assay

Apoptosis and cell cycle assay were performed at 24 h after indicated treatment for each group. The apoptosis rate was determined using Annexin V-FITC (fluorescein isothiocyanate) Apoptosis Kit (BD Biosciences, Franklin Lakes, NJ, USA) as per the manufacture's protocol. For cell cycle assay, the cells were fixed with 75% ethanol at 4°C overnight followed by supplementing with 500 μL PI/RNase Staining Buffer solution (BD Biosciences) for 30 minutes. The apoptosis rate and cell cycle were analyzed on a FACScan™ flow cytometry system.

Mice

C57BL/6 mice (eight-week-old, male) were purchased from Vital River (Beijing, China). All protocols involved animals were approved by the Animal Care and Use Committee of the Peking Union Medical College Hospital. All animal procedures were carried out in compliance with the National Research Council Guide for the Care and Use of Laboratory Animals.

Diabetic Nephropathy Modeling

C57BL/6 mice were randomly assigned to four groups (n=5): Control, streptozotocin (STZ) treatment, STZ+ 50 mg/kg CHR treatment, and STZ + 100 mg/kg CHR treatment. In order to induce diabetes, STZ (60 mg/kg body weight, Sigma-Aldrich) was intraperitoneally injected into mice according to previous references.[14,15] When the blood glucose of mice reached approximately 20 mmol/l, CHR (50 mg/kg or 100 mg/kg) was administered orally once daily. After 4 weeks of CHR treatment, urine samples were collected (within 24 h), and the mice were sacrificed to harvest kidneys and blood for further analysis.

Histology

Mouse kidney tissue blocks were fixed in 10% buffered formalin, dehydrated in graded ethanol, cleared in xylene, and embedded in paraffin. Serial sections were cut at 5 μm thickness. After deparaffinized and rehydrated, the sections were stained with hematoxylin-eosin (H&E) or Masson's trichrome. Inflammatory cell infiltration in the tissue sample was observed under a light microscope.

Detection of Serum Creatinine (CR) and Urea Nitrogen (BUN)

The levels of serum creatinine (CR) and blood urea nitrogen (BUN) were respectively quantified using Creatinine Assay Kit and Urea Assay Kit according to manufacturer's instructions (Nanjing Jiancheng Bioengineering Institute, Jiangsu, China).

Statistical Analysis

All experiments were performed as least in triplicates. All data were manifested as the mean ± standard deviation (SD). Difference among groups was determined by one-way analysis of variance (ANOVA) followed by Tukey's test. Data were statistically significant when $P < 0.05$. Statistical analyses were accomplished with GraphPad Prism 7.0 (GraphPad Software, San Diego, CA, USA).

Results

HG-Induced AB8/13 Cell Growth Inhibition Was Significantly Reversed by CHR

To test the cytotoxicity of CHR, CCK-8 assay was performed. As indicated in Figure 1A, 10, 20 or 40 μM CHR had no significant effect on cell viability, while 60 or 80 μM CHR exhibited notable cytotoxicity. Therefore, the non-toxic concentration of 40 μM CHR was selected for use in the following experiments. In addition, HG significantly decreased the viability of podocytes, while this phenomenon was obviously reversed by CHR (Figure 1B). Moreover, HG-induced inhibition of cell proliferation was notably reversed in the presence of CHR (Figure 1C). Altogether, HG-induced AB8/13 cell growth inhibition was significantly reversed by CHR.

CHR Inhibited the EMT Process in HG-Treated AB8/13 Cells in vitro

In order to investigate the effect of CHR on cell migration, transwell assay was used. As revealed in Figure 2A, 30 mM HG significantly promoted the migration of podocytes, while this phenomenon was partially reversed by CHR. In addition, the levels of TNF-α, IL-6 and IL-1β in supernatants of podocytes were notably upregulated by

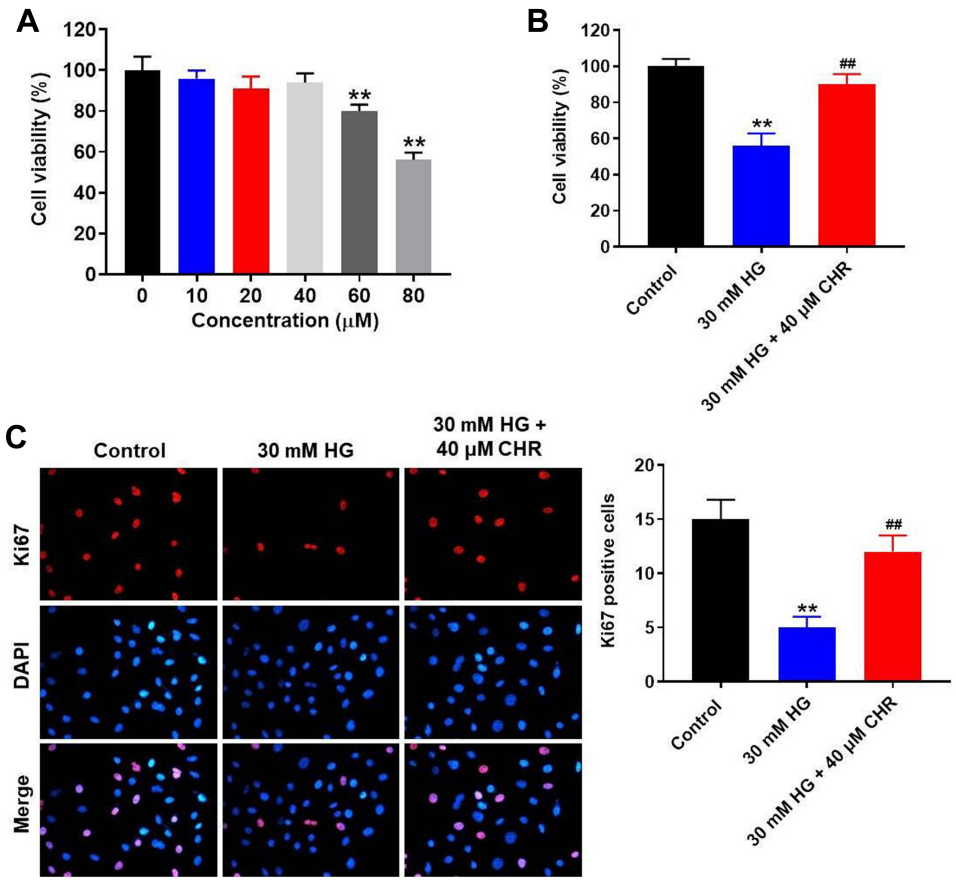

Figure 1 HG-induced AB8/13 cell growth inhibition was significantly reversed by CHR. (**A**) AB8/13 cells were treated with 10, 20, 40, 60 or 80 μM CHR. Then, cell viability was tested by CCK-8 assay. (**B**) AB8/13 cells were treated with 30 mM HG or 30 mM HG + 40 μM CHR. Then, cell viability was tested by CCK-8 assay. (**C**) The proliferation of AB8/13 cells was measured by Ki-67 staining. Red fluorescence indicates Ki-67. Blue fluorescence indicates DAPI. **P < 0.01 compared to control. ##P < 0.01 compared to 30 mM HG.

HG, while HG-induced increase of inflammatory responses was greatly inhibited by CHR (Figure 2B–D). Meanwhile, HG significantly increased the protein expressions of N-cadherin, α-SMA, Collagen III and Fibronectin in podocytes (Figure 2E). In contrast, the expression of E-cadherin in podocytes was notably inhibited by HG (Figure 2E). However, the effect of HG on these proteins was significantly reversed by CHR (Figure 2E). Taken together, CHR inhibited the EMT process in HG-treated AB8/13 cells in vitro.

CHR Alleviated HG-Induced Cytotoxicity in AB8/13 Cells via Inactivation of TGF-β Signaling

For the purpose of exploring the mechanism by which CHR mediated HG-induced cytotoxicity, Western blot was performed. As demonstrated in Figure 3A–D, the expressions of p-Smad2, p-Smad3 and p53 in podocytes were notably increased by HG, which was partially rescued in the presence of CHR. In contrast, HG greatly decreased the protein level of CDK2, while this phenomenon was obviously reversed by CHR (Figure 3A and E). Taken together, CHR alleviated HG-induced cytotoxicity in AB8/13 cells via inactivation of TGF-β signaling.

TGF-β Activator Reversed the Therapeutic Effect of CHR on HG-Treated AB8/13 Cells in vitro

To detect the cell apoptosis, flow cytometry was used. As expected, HG-induced cell apoptosis increase was significantly inhibited by CHR, while the anti-apoptotic effect of CHR was partially reversed in the presence of TGF-β activator (SRI-011381; N′-Cyclohexyl-N-(phenylmethyl)-N-(4-piperidinylmethyl)-urea) (Figure 4A). In addition, HG-induced activation of pro-apoptotic proteins (Bax and cleaved caspase 3) was significantly inhibited by

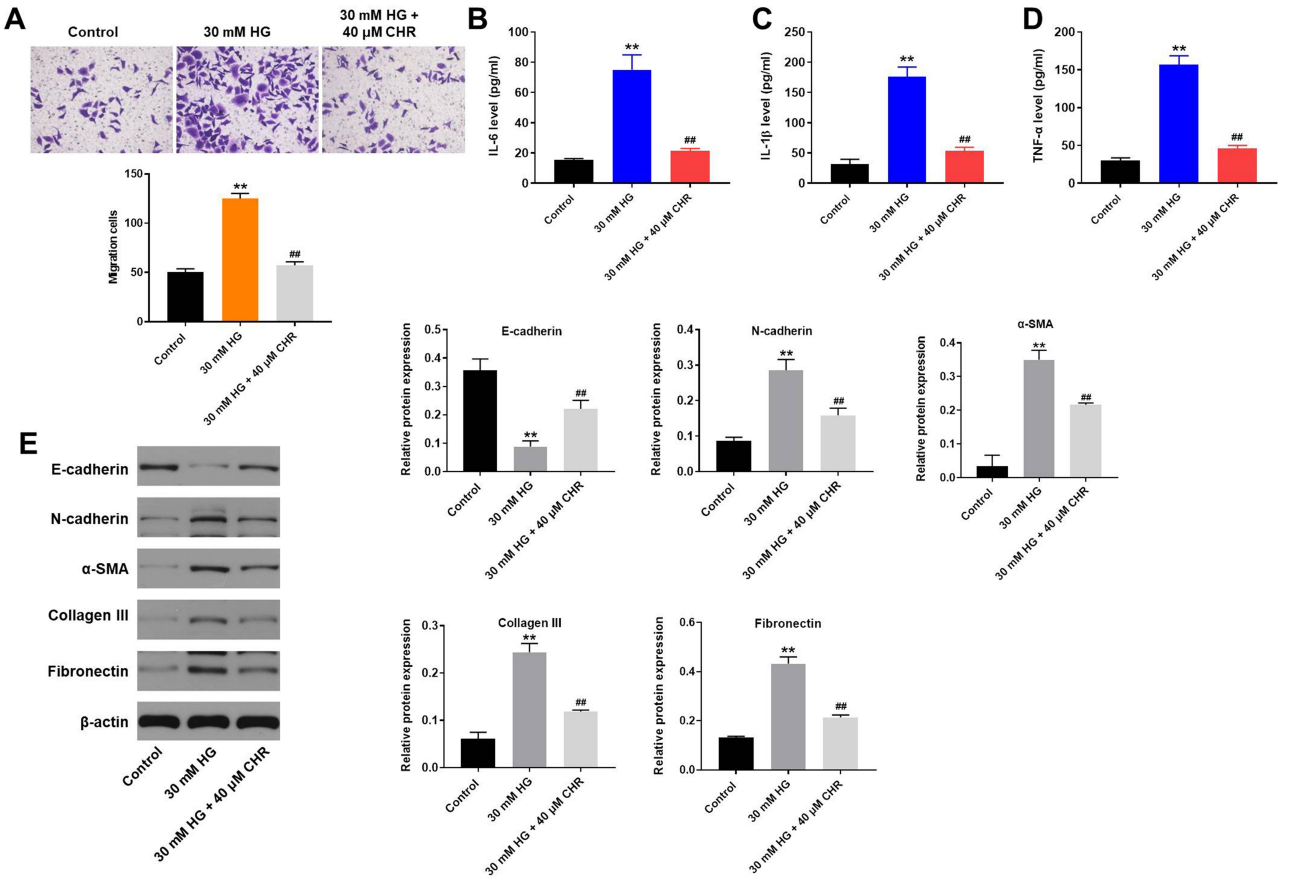

Figure 2 CHR inhibited the EMT process in HG-treated AB8/13 cells in vitro. (**A**) Cell migration was tested by transwell assay. (**B**–**D**) The levels of IL-6, IL-1β and TNF-α in supernatants of AB8/13 cells were detected by ELISA. (**E**) The protein expressions of E-cadherin, N-cadherin, α-SMA, Collagen III and Fibronectin in podocytes were detected by Western blot. The relative protein expressions were quantified by normalizing to β-actin. **P < 0.01 compared to control. ##P < 0.01 compared to 30 mM HG.

CHR as well (Figure 4B–D). Meanwhile, CHR partially reversed HG-induced inhibition of XIAP expression in podocytes (Figure 4B and E). However, the effect of CHR on these three proteins was significantly abolished in the presence of SRI-011381 (Figure 4B–E). Similarly, HG-induced G1 arrest in podocytes was significantly rescued by CHR, while the effect of CHR on cell cycle distribution was partially reversed by SRI-011381 (Figure 4F). To sum up, SRI-011381 reversed the therapeutic effect of CHR on HG-treated AB8/13 cells in vitro.

Anti-Apoptotic Effect of CHR in HG-Treated Podocytes Was Further Enhanced by TGF-β Inhibitor

To further confirm the mechanism by which CHR mediates HG-induced cytotoxicity in vitro, flow cytometry was performed. As indicated in Figure 5A, HG-induced increase of cell apoptosis was significantly inhibited by CHR, and the anti-apoptotic effect of CHR was further enhanced by LY2109761 (TGF-β inhibitor). In addition, the inhibitory effect of CHR on p-Smad2, p-Smad3 and cleaved caspase 3 in HG-treated podocytes were notably reversed by SRI-011381 (Figure 5B–E). In contrast, LY2109761 further increased the effect of CHR on these proteins (Figure 5B–E). Taken together, anti-apoptotic effect of CHR in HG-treated podocytes was further enhanced by TGF-β inhibitor.

CHR Significantly Alleviated the Symptom of DN in vivo

To investigate the effect of CHR on DN, in vivo model of DN was established. After treatment of STZ, mice exhibited loss of appetite and listlessness, while CHR alleviated these symptoms. As shown in Figure 6A, STZ significantly increase the blood glucose in mice; however, the increase of blood glucose was inhibited in the presence of CHR. In addition, inflammation infiltration and glomerular hypertrophy in kidney tissues of mice were observed after STZ treatment, while this phenomenon was greatly alleviated by 50 or 100 mg/kg CHR (Figure 6B). Consistently,

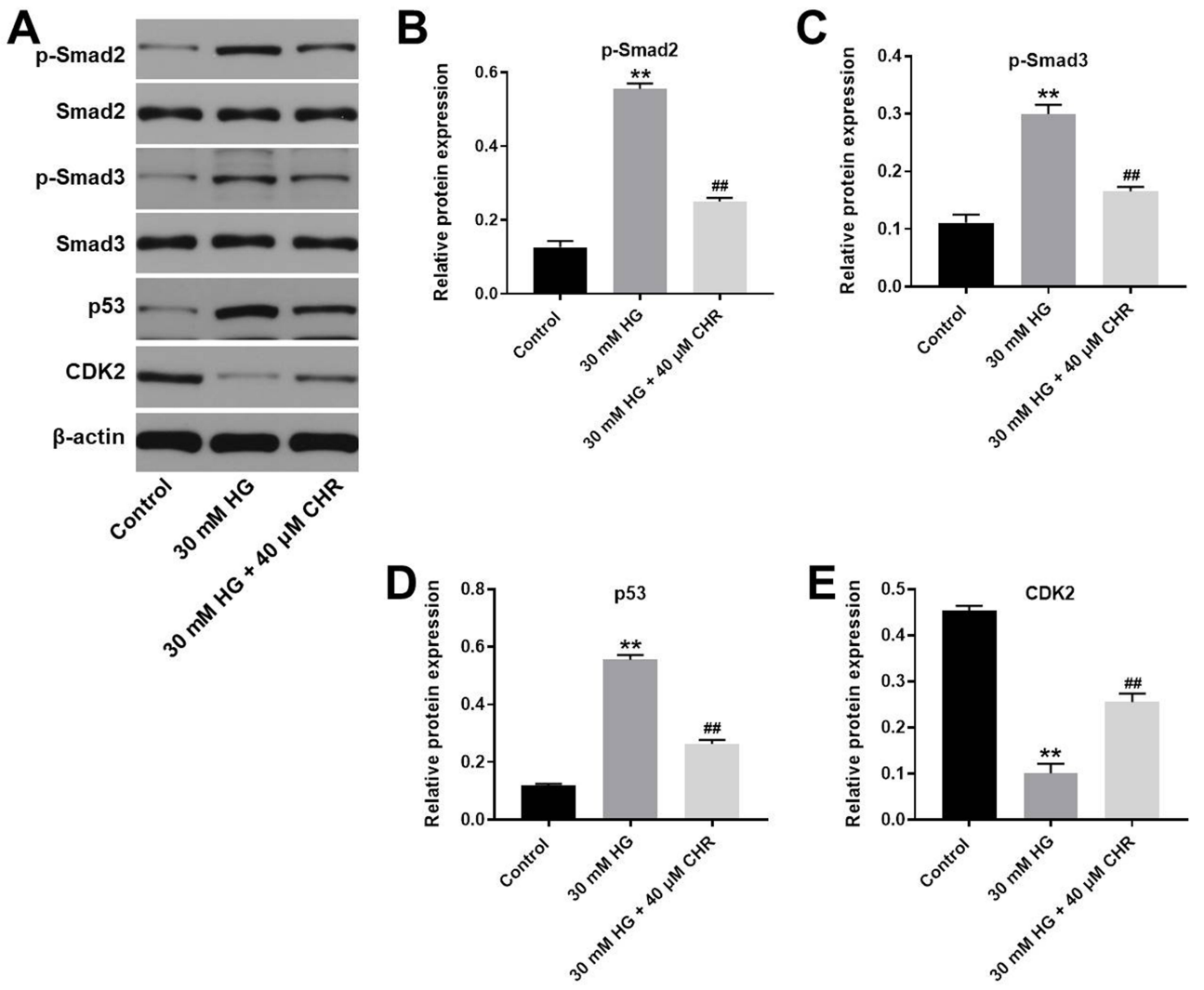

Figure 3 CHR alleviated HG-induced cytotoxicity in AB8/13 cells via inactivation of TGF-β signaling. (**A**) The protein expressions of Smad2, p-Smad2, Smad3, p-Smad3, p53 and CDK2 in podocytes were measured by Western blot. (**B**) The relative expression of p-Smad2 was quantified by normalizing to β-actin. (**C**) The relative expression of p-Smad3 was quantified by normalizing to β-actin. (**D**) The relative expression of p53 was quantified by normalizing to β-actin. (**E**) The relative expression of CDK2 was quantified by normalizing to β-actin. **P < 0.01 compared to control. ##P < 0.01 compared to 30 mM HG.

STZ-induced increase of fibrosis in tissues of mice was significantly reversed by 50 or 100 mg/kg CHR (Figure 6C). Moreover, CHR greatly inhibited STZ-induced increase of CR and BUN levels in serum of mice in a dose-dependent manner (Figure 6D and E). Furthermore, the expressions of α-SMA, Fibronectin, p-Smad2 and p-Smad3 in kidney tissues of mice were significantly increased by STZ, while the effect of STZ on these proteins was reversed by CHR (Figure 7A–E). In summary, CHR significantly alleviated the symptom of DN in vivo.

Discussion

CHR is one of traditional herb monomer extracted from plants of Rheum genus with few side effects. In this study, CHR significantly inhibited the progression of DN in vitro and in vivo. Chu et al found that CHR exhibited inhibitory effect on diabetes.[8] Our finding was similar to this previous report. In addition, our data supplemented the effect of CHR on DN, suggesting that CHR could serve as an anti-DN agent. Meanwhile, CHR could protect diabetic mice from myocardial injury via mediation of SIRT1/HMGB1/NF-κB signaling pathway.[16] However, our current study found CHR could mediate TGF-β signaling in DN. The difference may due to different types of diabetes complications.

In this research, CHR inhibited the progression of DN in vitro via inactivation of α-SMA, collagen III, N-cadherin

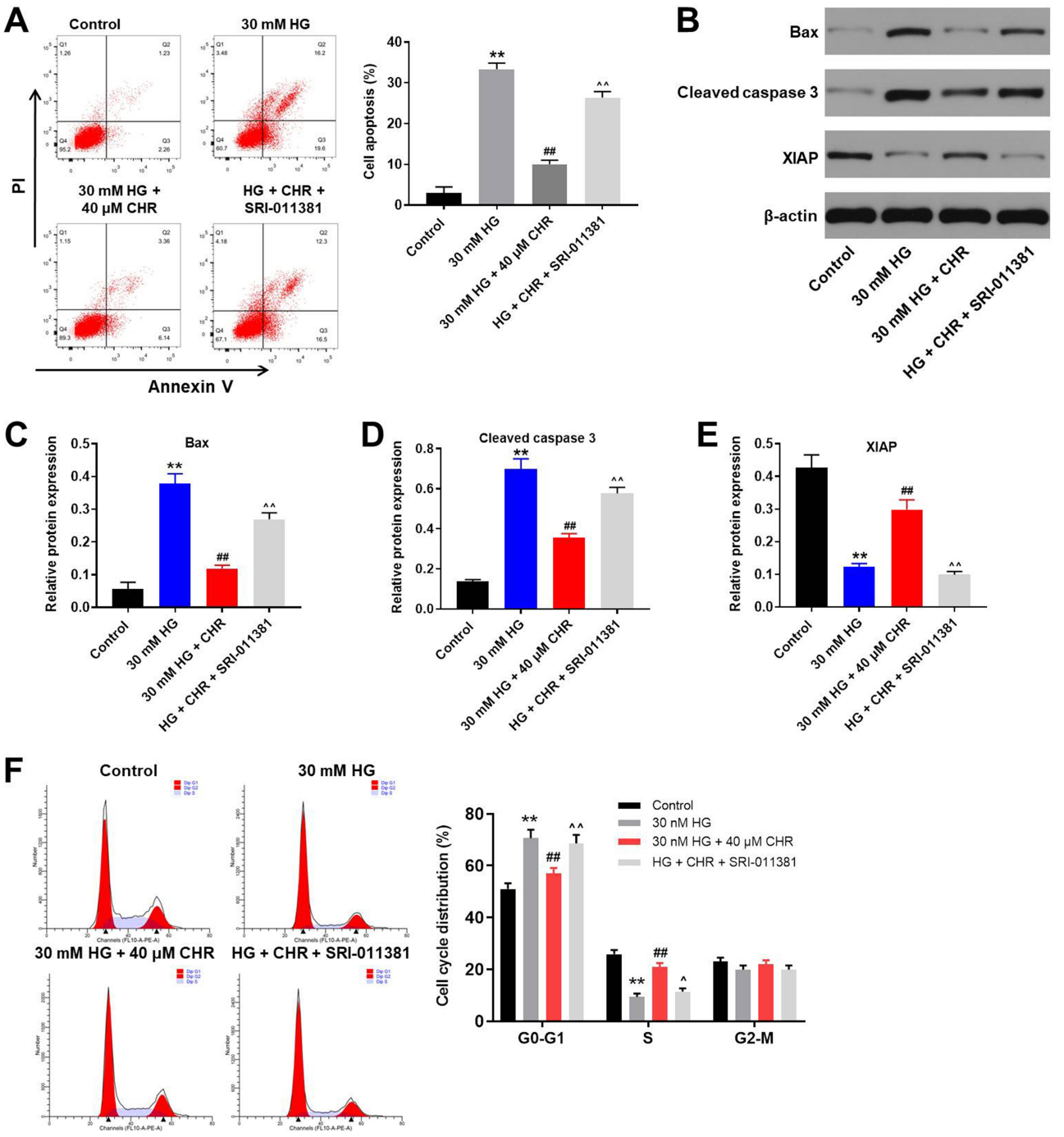

Figure 4 TGF-β activator reversed the therapeutic effect of CHR on HG-treated AB8/13 cells in vitro. (**A**) AB8/13 cells were treated with 30 mM HG, 30 mM HG + 40 μM CHR or 30 mM HG + 40 μM CHR + 10 ng/mL SRI-011381. The apoptosis of AB8/13 cells was detected by flow cytometry. (**B**) The protein expressions of Bax, XIAP and cleaved caspase 3 in podocytes were measured by Western blot. (**C**) The relative protein expression of Bax was quantified by normalizing to β-actin. (**D**) The relative expression of cleaved caspase 3 was quantified by normalizing to β-actin. (**E**) The relative expression of XIAP was quantified by normalizing to β-actin. (**F**) Cell cycle distribution was tested by flow cytometry. **P < 0.01 compared to control. ##P < 0.01 compared to 30 mM HG. ^P < 0.05, ^^P < 0.01 compared to 30 mM HG + 40 μM CHR.

and upregulation of E-cadherin. α-SMA, collagen III, N-cadherin and E-cadherin are known to be the key mediators in EMT process.[17–19] In addition, dysregulation of these proteins may lead to the regulation of EMT process.[20,21] The present study revealed that CHR could inhibit the development of CHR via inhibiting EMT process. Consistently, Deng et al found that CHR could suppress hypoxia-induced EMT process in colorectal cancer cells.[22] Based on these data, CHR could act as a mediator of EMT process in multiple diseases.

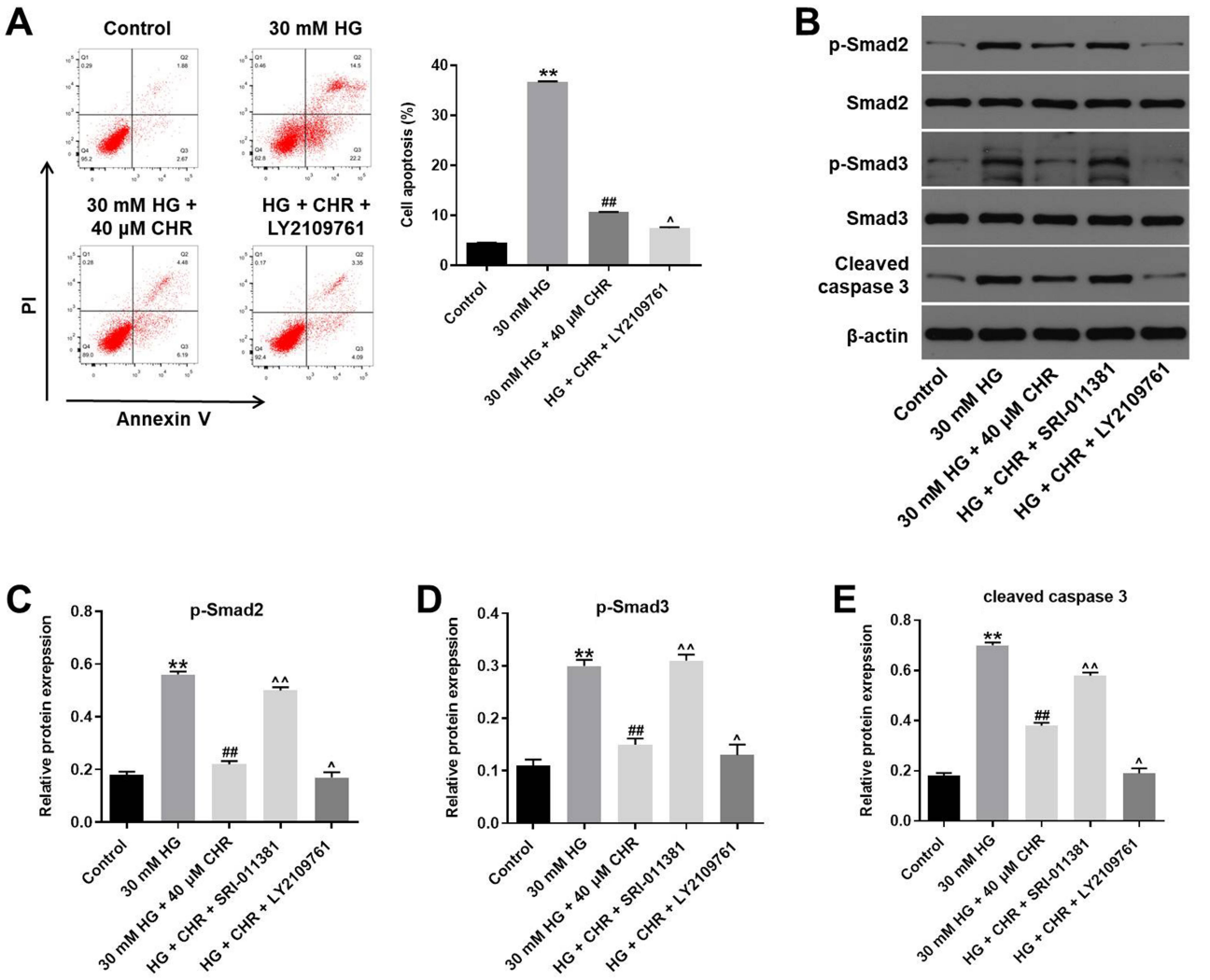

Figure 5 Anti-apoptotic effect of CHR in HG-treated podocytes was further enhanced by TGF-β inhibitor. (**A**) AB8/13 cells were treated with 30 mM HG, 30 mM HG + 40 μM CHR or 30 mM HG + 40 μM CHR + 10 ng/mL LY2109761. The apoptotic rate of AB8/13 cells was measured by flow cytometry. (**B**) The protein expressions of Smad2, Smad3, p-Smad2, p-Smad3 and cleaved caspase 3 in podocytes were detected by Western blot. (**C**–**E**) The relative expressions were quantified by normalizing to β-actin. **P < 0.01 compared to control. ##P < 0.01 compared to 30 mM HG. ^P < 0.05, ^^P < 0.01 compared to 30 mM HG + 40 μM CHR.

TGF-β signaling could serve as a key mediator in DN, and it was persistently upregulated in DN.[23,24] It has been confirmed that TGF-β can upregulate Smad-2/3 which can interference this pathway to affect the progression of DN.[25,26] In the present study, we found that CHR notably downregulated the p-smad2 and p-smad3 expressions in HG-induced podocytes. Based on these data, the mechanism underlying the anti-DN effects of CHR in vitro and in vivo was closely correlated with the inactivation of TGF-β1 signaling pathways. According to Moon et al, Gadd45β could inhibit the progression of renal fibrosis via downregulation of TGF-β.[27] TGF-β is considered as an important modulator in renal fibrosis.[28,29] Furthermore, DN could lead to renal fibrosis.[30,31] Therefore, the similarity between our data and this report may result from the association between DN and renal fibrosis. Besides, upregulation of TGF-β1 signaling could promote the EMT process in some diseases.[32,33] Our findings were consistent to these data, indicating that CHR could alleviate the symptom of DN via inactivation of TGF-β/EMT signaling pathway.

P53 and CDK2 are known to be key mediators in cell cycle distribution.[34,35] In addition, upregulation of p53 could lead to G1 phase arrest in cells.[36,37] A previous report found that Smad3 promotes acute kidney injury (AKI) sensitivity in diabetic mice via binding to p53.[38] Similarly, our data revealed that CHR suppressed the development of DN via mediation of Smad3/p53/CDK2 axis.

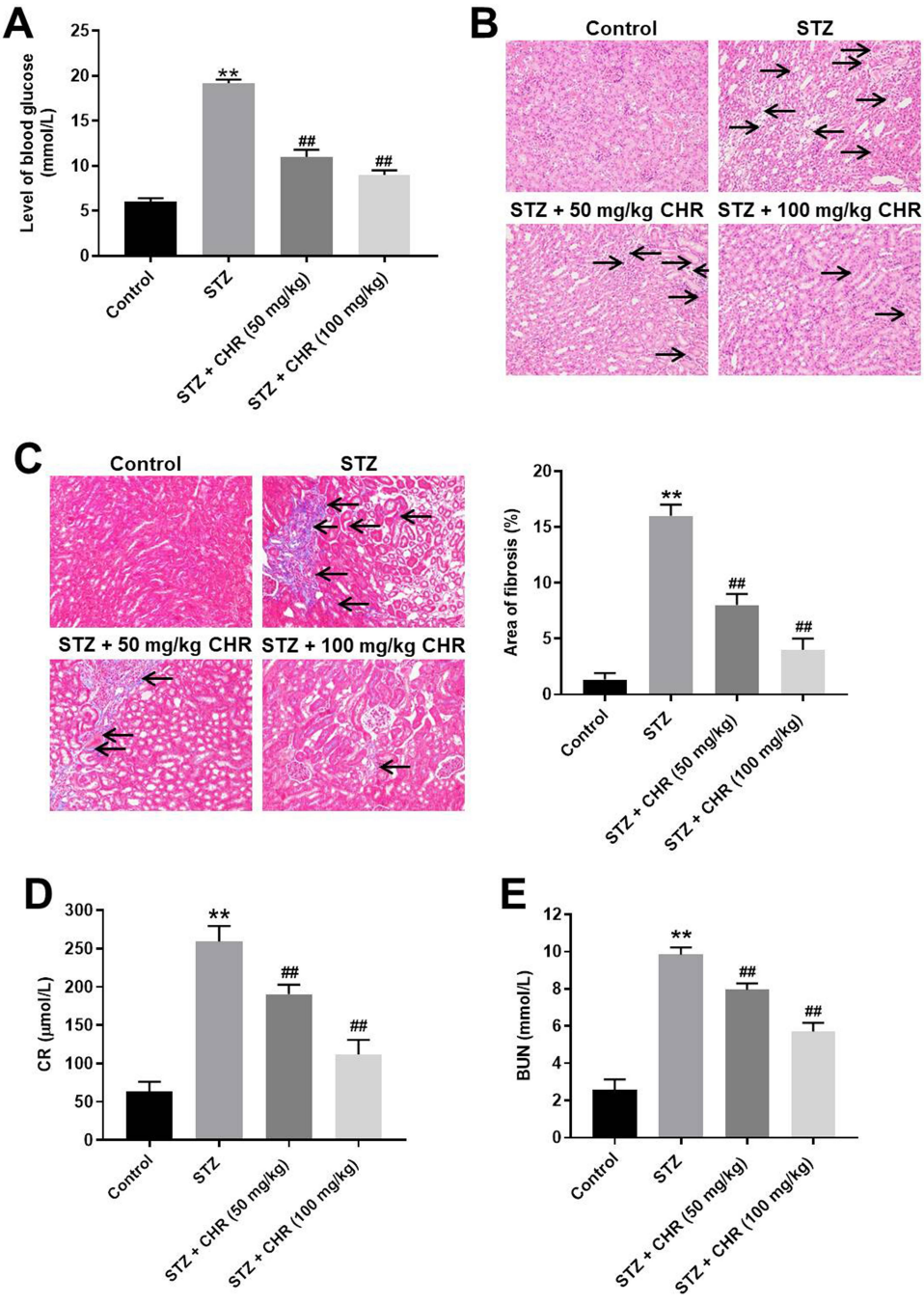

Figure 6 CHR significantly alleviated the symptom of DN in vivo. (**A**) The level of blood glucose in mice was tested. (**B**) H&E staining of mice kidney tissue in control, STZ, STZ + 50 mg/kg CHR or STZ + 100 mg/kg CHR group were detected. Black arrow indicates glomerular hypertrophy or inflammation infiltration. (**C**) Masson staining of mice kidney tissue in control, STZ, STZ + 50 mg/kg CHR or STZ + 100 mg/kg CHR group was detected. The rate of fibrosis in mice was quantified. Black arrow indicates collagen fibers. (**D**) The level of CR in serum of mice was measured by Creatinine Assay kit. (**E**) The level of BUN in serum of mice was measured by Urea Assay Kit. **P < 0.01 compared to control. ##P < 0.01 compared to STZ.

Of course, there are some limitations in this study as follows: (1) the detailed mechanism by which CHR mediates TGF-β signaling is unclear; (2) this research only focused on TGF-β signaling so far. Thereby, more investigations are needed in the future.

In conclusion, CHR inhibited the progression of DN via inactivation of TGF-β/EMT signaling. Our findings were helpful to uncover the mechanism by which CHR regulates DN, as well as inspire the development of novel therapy against DN.

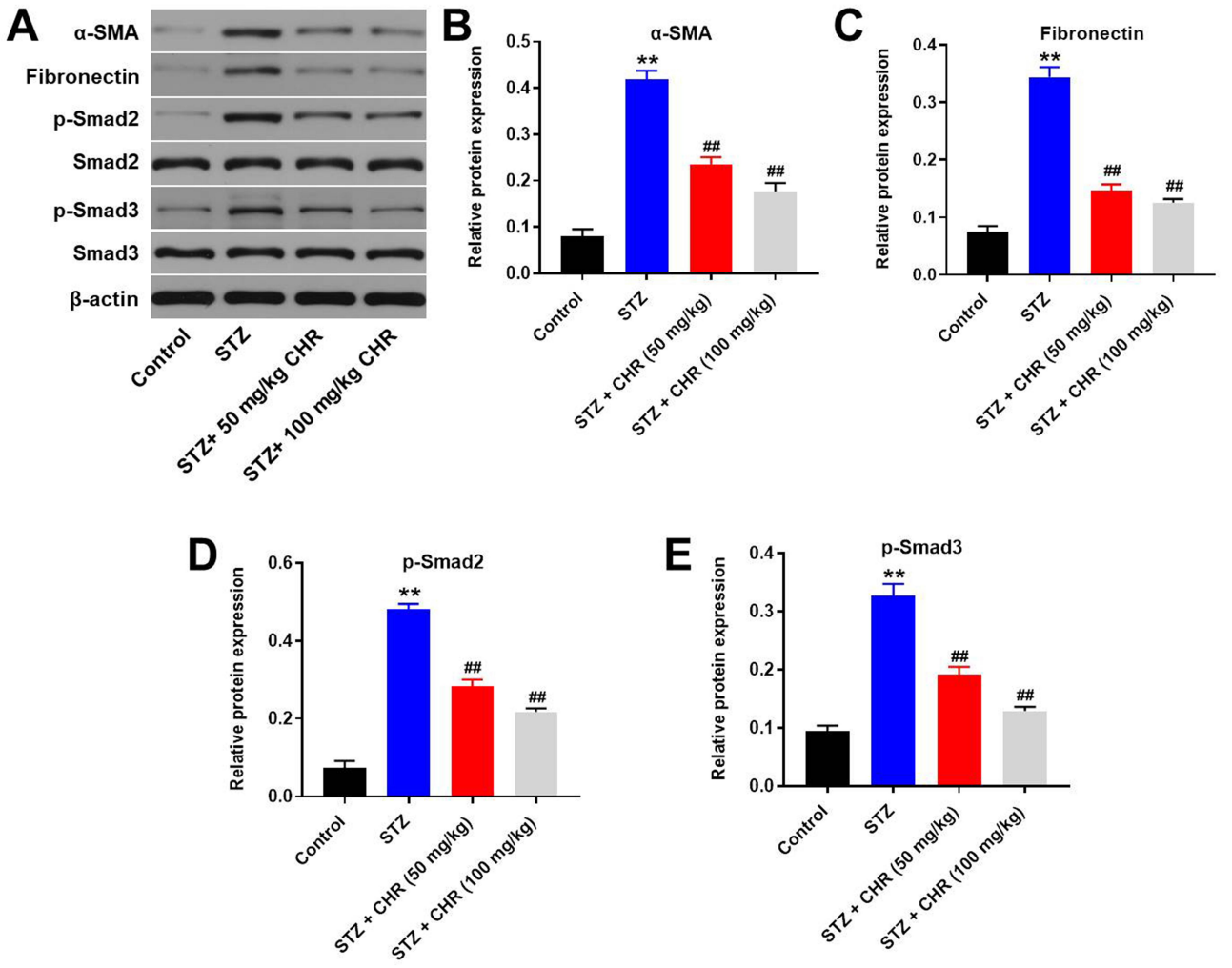

Figure 7 CHR attenuated the symptom of DN via downregulation of TGF-β signaling. (**A**) The protein expressions of α-SMA, Fibronectin, Smad2, p-Smad2, Smad3 and p-Smad3 in podocytes were measured by Western blot. (**B**) The relative expression of α-SMA was quantified by normalizing to β-actin. (**C**) The relative expression of Fibronectin was quantified by normalizing to β-actin. (**D**) The relative expression of p-Smad2 was quantified by normalizing to β-actin. (**E**) The relative expression of p-Smad3 was quantified by normalizing to β-actin. **P < 0.01 compared to control. ##P < 0.01 compared to STZ.

Funding

This work was supported by Foundation of National Natural Science (No. 81573921).

Disclosure

The authors declared no competing interests in this research.

References

1. Bhaskaran SP, Huang T, Rajendran BK. et al. Ethnic-specific BRCA1/2 variation within Asia population: evidence from over 78 000 cancer and 40 000 non-cancer cases of Indian, Chinese, Korean and Japanese populations. *J Med Genet*.2020:jmedgenet-2020-107299. doi:10.1136/jmedgenet-2020-107299
2. Temurer Afsar Z, Aycicek B, Tutuncu Y, Cavdar U, Sennaroglu E. Relationships between microvascular complications of diabetes mellitus and levels of macro and trace elements. *Minerva Endocrinol*. 2020.
3. Bhatia D, Choi ME. Autophagy in kidney disease: advances and therapeutic potential. *Prog Mol Biol Transl Sci*. 2020;172:107–133.
4. Cai R, Jiang J. LncRNA ANRIL silencing alleviates high glucose-induced inflammation, oxidative stress, and apoptosis via upregulation of MME in podocytes. *Inflammation*. 2020;43(6):2147–2155. doi:10.1007/s10753-020-01282-1
5. Huang L, Lin T, Shi M, Chen X, Wu P. Liraglutide suppresses production of extracellular matrix proteins and ameliorates renal injury of diabetic nephropathy by enhancing Wnt/beta-catenin signaling. *Am J Physiol Renal Physiol*. 2020;319(3):F458–F468. doi:10.1152/ajprenal.00128.2020
6. Hsu PC, Cheng CF, Hsieh PC, et al. Chrysophanol regulates cell death, metastasis, and reactive oxygen species production in oral cancer cell lines. *Evid Based Complement Alternat Med*. 2020;2020:5867064. doi:10.1155/2020/5867064
7. Dou F, Ding Y, Wang C, et al. Chrysophanol ameliorates renal interstitial fibrosis by inhibiting the TGF-beta/Smad signaling pathway. *Biochem Pharmacol*. 2020;180:114079. doi:10.1016/j.bcp.2020.114079
8. Chu X, Zhou S, Sun R, et al. Chrysophanol relieves cognition deficits and neuronal loss through inhibition of inflammation in diabetic mice. *Neurochem Res*. 2018;43(4):972–983. doi:10.1007/s11064-018-2503-1

9. Duan XJ, Zhang X, Li LR, Zhang JY, Chen YP. MiR-200a and miR-200b restrain inflammation by targeting ORMDL3 to regulate the ERK/MMP-9 pathway in asthma. *Exp Lung Res*. 2020;46 (9):321–331. doi:10.1080/01902148.2020.1778816
10. Shi Y, Huang C, Zhao Y, et al. RIPK3 blockade attenuates tubulointerstitial fibrosis in a mouse model of diabetic nephropathy. *Sci Rep*. 2020;10(1):10458. doi:10.1038/s41598-020-67054-x
11. Fan Z, Qi X, Yang W, Xia L, Wu Y. Melatonin ameliorates renal fibrosis though the inhibition of NF-kappaB and TGF-beta1/Smad3 pathways in db/db diabetic mice. *Arch Med Res*. 2020;51 (6):524–534. doi:10.1016/j.arcmed.2020.05.008
12. Rao N, Wang X, Xie J, et al. Stem cells from human exfoliated deciduous teeth ameliorate diabetic nephropathy in vivo and in vitro by inhibiting advanced glycation end product-activated epithelial-mesenchymal transition. *Stem Cells Int*. 2019;20 19:2751475. doi:10.1155/2019/2751475
13. Lin S, Yu L, Ni Y, et al. Fibroblast growth factor 21 attenuates diabetes-induced renal fibrosis by negatively regulating TGF-beta-p53-Smad2/3-mediated epithelial-to-mesenchymal transition via activation of AKT. *Diabetes Metab J*. 2020;44(1):158–172. doi:10.4093/dmj.2018.0235
14. Nalin N, Dhanhani AA, AlBawardi A, et al. The effect of angiotensin II on diabetic glomerular hyperpermeability: in vivo permeability studies in rats. *Am J Physiol Renal Physiol*. 2020. doi:10.1152/ajprenal.00259.2020
15. Thisted L, Ostergaard MV, Pedersen AA, et al. Rat pancreatectomy combined with isoprenaline or uninephrectomy as models of diabetic cardiomyopathy or nephropathy. *Sci Rep*. 2020;10(1):16130. doi:10.1038/s41598-020-73046-8
16. Xue P, Zhao J, Zheng A, et al. Chrysophanol alleviates myocardial injury in diabetic db/db mice by regulating the SIRT1/HMGB1/NF-kappaB signaling pathway. *Exp Ther Med*. 2019;18(6):4406–4412.
17. Wang G, Zhou Y, Chen W, et al. miR-21-5p promotes lung adenocarcinoma cell proliferation, migration and invasion via targeting WWC2. *Cancer Biomark*. 2020;28(4):549–559. doi:10.3233/CBM-201489
18. Jahani M, Khanahmad H, Nikpour P. Evaluation of the effects of valproic acid treatment on cell survival and epithelial-mesenchymal transition-related features of human gastric cancer cells. *J Gastrointest Cancer*. 2020. doi:10.1007/s12029-019-00332-8
19. Zhang X, Zou Y, Liu Y, et al. Inhibition of PIM1 kinase attenuates bleomycin-induced pulmonary fibrosis in mice by modulating the ZEB1/E-cadherin pathway in alveolar epithelial cells. *Mol Immunol*. 2020;125:15–22. doi:10.1016/j.molimm.2020.06.013
20. Peng J, Wu HJ, Zhang HF, Fang SQ, Zeng R. miR-143-3p inhibits proliferation and invasion of hepatocellular carcinoma cells by regulating its target gene FGF1. *Clin Transl Oncol*. 2020. doi:10.1007/s12094-020-02440-5
21. Hernandez-Padilla L, Reyes de la Cruz H, Campos-Garcia J. Antiproliferative effect of bacterial cyclodipeptides in the HeLa line of human cervical cancer reveals multiple protein kinase targeting, including mTORC1/C2 complex inhibition in a TSC1/2-dependent manner. *Apoptosis*. 2020;25(9–10):632–647. doi:10.1007/s10495-020-01619-z
22. Deng M, Xue YJ, Xu LR, et al. Chrysophanol suppresses hypoxia-induced epithelial-mesenchymal transition in colorectal cancer cells. *Anat Rec (Hoboken)*. 2019;302(9):1561–1570. doi:10.1002/ar.24081
23. Jin S, Li J, Barati M, et al. Loss of NF-E2 expression contributes to the induction of profibrotic signaling in diabetic kidneys. *Life Sci*. 2020;254:117783. doi:10.1016/j.lfs.2020.117783
24. Zheng XP, Nie Q, Feng J, et al. Kidney-targeted baicalin-lysozyme conjugate ameliorates renal fibrosis in rats with diabetic nephropathy induced by streptozotocin. *BMC Nephrol*. 2020;21(1):174. doi:10.1186/s12882-020-01833-6
25. Cappelli C, Tellez A, Jara C, et al. The TGF-beta profibrotic cascade targets ecto-5′-nucleotidase gene in proximal tubule epithelial cells and is a traceable marker of progressive diabetic kidney disease. *Biochim Biophys Acta Mol Basis Dis*. 2020;1866(7):165796. doi:10.1016/j.bbadis.2020.165796
26. Verzola D, Milanesi S, Viazzi F, et al. Enhanced myostatin expression and signalling promote tubulointerstitial inflammation in diabetic nephropathy. *Sci Rep*. 2020;10(1):6343. doi:10.1038/s41598-020-62875-2
27. Moon SJ, Kim JH, Choi YK, Lee CH, Hwang JH. Ablation of Gadd45beta ameliorates the inflammation and renal fibrosis caused by unilateral ureteral obstruction. *J Cell Mol Med*. 2020;24 (15):8814–8825. doi:10.1111/jcmm.15519
28. Zhang W, Li X, Tang Y, et al. miR-155-5p implicates in the pathogenesis of renal fibrosis via targeting SOCS1 and SOCS6. *Oxid Med Cell Longev*. 2020;2020:6263921.
29. Jiang Y, Zhu Y, Zhen T, et al. Transcriptomic analysis of the mechanisms of alleviating renal interstitial fibrosis using the traditional Chinese medicine Kangxianling in a rat model. *Sci Rep*. 2020;10 (1):10682. doi:10.1038/s41598-020-67690-3
30. Sun J, Wang J, Lu W, et al. MiR-325-3p inhibits renal inflammation and fibrosis by targeting CCL19 in diabetic nephropathy. *Clin Exp Pharmacol Physiol*. 2020. doi:10.1111/1440-1681.13371
31. Yang J, Dong H, Wang Y, et al. Cordyceps cicadae polysaccharides ameliorated renal interstitial fibrosis in diabetic nephropathy rats by repressing inflammation and modulating gut microbiota dysbiosis. *Int J Biol Macromol*. 2020;163:442–456. doi:10.1016/j.ijbiomac.2020.06.153
32. Peng R, Chen Y, Wei L, et al. Resistance to FGFR1-targeted therapy leads to autophagy via TAK1/AMPK activation in gastric cancer. *Gastric Cancer*. 2020;23(6):988–1002. doi:10.1007/s10120-020-01088-y
33. Sari E, Oztay F, Tasci AE. Vitamin D modulates E-cadherin turnover by regulating TGF-beta and Wnt signalings during EMT-mediated myofibroblast differentiation in A459 cells. *J Steroid Biochem Mol Biol*. 2020;202:105723. doi:10.1016/j.jsbmb.2020.105723
34. Bakshi HA, Zoubi MSA, Faruck HL, et al. Dietary crocin is protective in pancreatic cancer while reducing radiation-induced hepatic oxidative damage. *Nutrients*. 2020;12(6):1901. doi:10.3390/nu12061901
35. Umar S, Soni R, Durgapal SD, Soman S, Balakrishnan S. A synthetic coumarin derivative (4-flourophenylacetamide-acetyl coumarin) impedes cell cycle at G0/G1 stage, induces apoptosis, and inhibits metastasis via ROS-mediated p53 and AKT signaling pathways in A549 cells. *J Biochem Mol Toxicol*. 2020;e22553.
36. Smith HL, Southgate H, Tweddle DA, Curtin NJ. DNA damage checkpoint kinases in cancer. *Expert Rev Mol Med*. 2020;22:e2. doi:10.1017/erm.2020.3
37. Liu JY, Fu WQ, Zheng XJ, et al. Avasimibe exerts anticancer effects on human glioblastoma cells via inducing cell apoptosis and cell cycle arrest. *Acta Pharmacol Sin*. 2020.
38. Wang JN, Yang Q, Yang C, et al. Smad3 promotes AKI sensitivity in diabetic mice via interaction with p53 and induction of NOX4-dependent ROS production. *Redox Biol*. 2020;32:101479. doi:10.1016/j.redox.2020.101479